

# Transition from the Bose gas to the Fermi gas through a Nuclear Halo

V.P. Maslov <sup>\*</sup>

## Abstract

The first part of the paper deals with the behavior of the Bose–Einstein distribution as the activity  $a \rightarrow 0$ . In particular, the neighborhood of the point  $a = 0$  is studied in great detail, and the expansion of both the Bose distribution and the Fermi distribution in powers of the parameter  $a$  is used.

This approach allows to find the value of the parameter  $a_0$ , for which the Bose distribution (in the statistical sense) becomes zero.

In the second part of the paper, the process of separation of a nucleon from the atom’s nucleus is studied from the mathematical point of view. At the moment when the nucleon tears away from the fermionic nucleus, the nucleus becomes a boson. We investigate the further transformations of bosonic and fermionic separation states in a small neighborhood of the pressure  $P$  equal to zero. We use infinitely small quantities to modify the parastatistical distribution. Our conception is based on interpolation formulas yielding expansions in powers of the density. This method differs from those in other models based on the interaction potential between two or three particles.

We obtain new important relations connecting the temperature with the chemical potential during the separation of a nucleon from the atom’s nucleus. The obtained relations allow us to construct, on an antipode of sorts of the Hougen–Watson P-Z chart, the very high temperature isotherms corresponding to nuclear matter. It is proved mathematically that the passage of particles satisfying the Fermi–Dirac distribution to the Bose–Einstein distribution in the neighborhood of pressure  $P$  equal to zero occurs in a region known as the “halo”.

## 1 Statistical transition of the Bose gas to the Fermi gas

1. It is well known that a Bose particle consists of two bound Fermi particles. For a Bose particle to become a Fermi particle, it is necessary that one of the Fermi particles forming the Bose particle must be “pushed out” *beyond* the volume  $V$  under consideration (in the two-dimensional case,  $V$  is the area) under the action of some energy. In the case of the volume of a ball (the area of a disk), the radius  $r$  is the radius of the “shell,” outside which the “entanglement” of two fermions into one boson terminates according to the Einstein–Podolsky–Rosen concept.

Let there be given a macroscopic volume  $V$  of radius at least 1 mm filled completely with a Bose gas (for example, helium-4) for the activity  $a = 1$ , i.e., on the caustic. We shall

---

<sup>\*</sup>National Research University Higher School of Economics, Moscow, 123458, Russia; Moscow State University, Physics Faculty, Moscow, 119234, Russia

determine what amount of energy is required to “push out” one fermion from the specific volume under consideration. To obtain the total energy, i.e., the energy needed for the Bose gas (for example, helium-4) to go over completely into the Fermi gas (for example, helium-3), we must multiply the resulting quantity by the number of particles in the gas. It is the amount of energy required for the transition of the Bose gas to the Fermi gas that is the subject of the present study. In particular, we shall show that, for the number of degrees of freedom  $D > 2$ , we will have a jump of the energy  $E$  at the point  $E = 1/\log a$  for  $a = 0$ , where  $a$  is the activity,

*Remark 1.* “The barrier” formed by the shell is described by a Bardeen–Cooper–Schrieffer type equation for Cooper pairs [1]–[2]. Since the volume under consideration is macroscopic (at least  $1 \text{ mm}^3$ ), by statistical calculations, the shell far exceeds the volume of the nucleus.

In our conception, we use the polylogarithm. The polylogarithm is determined by the activity  $a$  and the number of degrees of freedom  $D$ , where  $D = 2\gamma + 2$  and  $\gamma$  is an auxiliary parameter. In the two-dimensional case,  $\gamma = 0$ , while, in the general number theory,  $\gamma \leq 0$ . The positive value  $\gamma > 0$  corresponds to the gas state in classical thermodynamics and  $\gamma < 0$ , to the liquid state.

Both parameters  $a$  and  $D$  are dimensionless, while the volume  $V$  is a dimensional parameter. The dimensionless small parameter

$$\frac{\hbar^2}{mVT} \quad (1)$$

for  $\gamma = 0$  (in the two-dimensional case,  $V$  is the area) corresponds to the semiclassical approximation in the sense that the semiclassical asymptotics is expanded in terms of this parameter. Therefore, as a rule, a parameter  $\lambda$  is also added so that the multiplicative term before the polylogarithm becomes dimensionless. Statistical quantities divided by the number of particles i.e., belonging to one particle, are called *specific quantities*:  $V/N$  is the *specific volume* and  $E/N$  is the *specific energy*. We proceed as follows: first, we shall find the specific energy and, further, we shall multiply it by the number of particles on the caustic  $a = 1$ .

The quantity  $PV/(NT)$ , where  $P$  is the pressure and  $T$  is the temperature, is dimensionless. It is called the *compressibility factor*. The temperature  $T$  in the two-dimensional case is determined from the relation  $M = T \text{Li}_2(a)$ , where  $a = 1$ , as

$$T = \sqrt{\frac{M}{\zeta(2)}}, \quad (2)$$

where  $\zeta(\cdot)$  is the Riemann zeta-function.

For the number of degrees of freedom  $D > 2$ , the density of the Bose gas at the point  $a = 0$  vanishes as  $1/|\log a|$  and behaves as  $1/\log a$  for the Fermi gas (see below), just as the energy  $E$  of the Bose gas. The coefficient of  $1/\log a$  for the energy of the Bose gas allows us to determine the energy needed for “all” the Bose particles to go over into Fermi particles.

The hidden parameter appearing in the Einstein–Podolsky–Rosen paradox could unite quantum and classical mechanics in the sense defined by the author; it can be obtained from the general arguments in the first chapter of the book [3]. After Sec. 4 “Role of Energy,” the most important notion of time is introduced in Sec. 5 “Statistical Matrix.” Since, in the present paper, we calculate the statistical energy  $\Delta E$  required for the transition of the Bose gas into the Fermi gas, it follows that by using Sec. 5 of the book [3] we can also calculate the statistical time

$$\Delta t \sim \frac{\hbar}{\Delta E}, \quad (3)$$

given by the authors of [3] to explain the transition to macroscopic physics. From the point of view of the metamathematical hidden parameter, this time plays a role similar to that of the mean free time in classical mechanics.

Let  $k$  denote the maximal admissible number of particles that can occupy one energy level, and let  $N_i$  denote the number of particles located at the  $i$ th energy level <sup>1</sup>. The number  $k$  is the maximal number of particles located at one energy level of a quantum operator of the Hamiltonian  $\hat{H}$ . For a Bose systems, it is obvious that  $N_i \leq N$ . Therefore, for a Bose system,  $k \leq N$ .

On the other hand, the number  $N_i$  is arbitrarily large, more precisely, maximally large, in view of the inequality  $N_i \leq N$ . This implies that  $k = N$ , and we obtain an equation for  $N$  in which, on the left-hand and right-hand sides, we have  $N$  from the formula for the Gentile parastatistics (see Sec. 4 below).

**2.** To find the energy that is of interest to us (the energy of transition of Bose particles to Fermi particles), it suffices to study the transition at the point  $a = 0$ . If we wish to widen the interval of the jump from the Bose distribution to the Fermi distribution, then we must use parastatistics, or Gentile statistics [6] in which the first term in parentheses gives the distribution for Bose particles and the other term, the parastatistical correction. The corresponding formula in the three-dimensional case is of the form (see [7])

$$N = \lambda \left\{ \int_0^\infty \frac{p^2 dp}{\exp\{p^2/2mT\} - 1} - (k+1) \int_0^\infty \frac{p^2 dp}{\exp\{(k+1)p^2/2mT\} - 1} \right\}. \quad (4)$$

For the Bose–Einstein distribution in the case of  $D$  degrees of freedom the following formulas are valid:

$$E = T\Phi(\gamma + 1)Li_{2+\gamma}(a), \quad N = \Phi Li_{1+\gamma}(a). \quad (5)$$

Here and elsewhere,  $\gamma = D/2 - 1$ ,  $T$  is the temperature,  $a = e^{\mu/T}$  is the activity,  $\mu$  is the chemical potential,

$$\Phi = \left( \frac{\sqrt{2\pi mT}}{2\pi\hbar} \right)^{2(\gamma+1)} V,$$

where  $m$  is the mass of one particle,  $V$  is the volume of the system of particles, and  $\hbar$  is the Planck constant.

For the Fermi–Dirac distribution, the following formulas hold:

$$E = -T\Phi(\gamma + 1)Li_{2+\gamma}(-a), \quad N = -\Phi Li_{1+\gamma}(-a). \quad (6)$$

As we see, formulas (5) and (6) differ by sign; therefore, the activity  $a$  passes through the point  $a = 0$ .

In the case of parastatistics, i.e., there are at most  $k$  particles at each level, the following relations hold:

$$E = \Phi T(\gamma + 1)(Li_{2+\gamma}(a) - \frac{1}{(k+1)^{\gamma+1}} Li_{2+\gamma}(a^{k+1})), \quad (7)$$

$$N = \Phi(Li_{1+\gamma}(a) - \frac{1}{(k+1)^\gamma} Li_{1+\gamma}(a^{k+1})). \quad (8)$$

According to the conventional definitions, for  $k = 1$ , we have the Fermi case and, for  $k = \infty$ , the Bose case.

---

<sup>1</sup>For the transition from a discrete spectrum to a continuous one with respect to the parameter  $V$ , see [4], [5].

Let us consider another important dimensionless quantity, which was mentioned above, namely, the compressibility factor defined by the formula  $Z = PV/NT$ .

The following thermodynamic relation is well known:

$$E = -(\gamma + 1)\Omega = PV(\gamma + 1) \quad (9)$$

As is seen from relation (9),  $PV$  is expressed in terms of  $E$ ; therefore, the compressibility factor can be expressed in terms of the polylogarithm. For the Bose case, the compressibility factor takes the form

$$Z|_{\text{Bose}} = \frac{Li_{2+\gamma}(a)}{Li_{1+\gamma}(a)} \quad (10)$$

and, for the Fermi case, we have

$$Z|_{\text{Fermi}} = \frac{Li_{2+\gamma}(-a)}{Li_{1+\gamma}(-a)}. \quad (11)$$

For the Gentile statistics with parameter  $k$ , we have the following expression for the compressibility factor:

$$Z|_k = \frac{Li_{2+\gamma}(a) - \frac{1}{(k+1)^{\gamma+1}} Li_{2+\gamma}(a^{k+1})}{Li_{1+\gamma}(a) - \frac{1}{(k+1)^{\gamma}} Li_{1+\gamma}(a^{k+1})}. \quad (12)$$

**3.** The compressibility factor  $Z$  multiplied by the temperature  $T$  is the specific energy. To obtain the jump of the specific energy, it suffices to consider the jump of the compressibility factor from the Fermi system to the Bose system.

The following representation for the polylogarithm is known:

$$Li_s(a) = \sum_{i=1}^{\infty} \frac{a^i}{i^s}; \quad (13)$$

substituting this expression into (10), (11), (12), we obtain the following expansions of the compressibility factor:

$$\begin{aligned} Z|_{\text{Fermi}} = & 1 + a2^{-\gamma-2} - a^22^{-2\gamma-3}3^{-\gamma-2}(2^{2\gamma+4} - 3^{\gamma+2}) \\ & - a^32^{-3\gamma-4}3^{-\gamma-2}(7 \cdot 2^{2\gamma+2} - 3^{\gamma+2} - 2^{\gamma}3^{\gamma+3}) \\ & - a^42^{-4\gamma-5}3^{-2\gamma-3}5^{-\gamma-2}(2^{4\gamma+7}3^{2\gamma+3} - 2^{4\gamma+6}5^{\gamma+2} - 3^{2\gamma+3}5^{\gamma+2} + 2^{2\gamma+3}3^{\gamma+1}5^{\gamma+3} - 2^{\gamma}3^{2\gamma+3}5^{\gamma+3}) \\ & + O(a^5), \end{aligned} \quad (14)$$

$$\begin{aligned} Z|_{\text{Bose}} = & 1 - a2^{-\gamma-2} - a^22^{-2\gamma-3}3^{-\gamma-2}(2^{2\gamma+4} - 3^{\gamma+2}) \\ & + a^32^{-3\gamma-4}3^{-\gamma-2}(7 \cdot 2^{2\gamma+2} - 3^{\gamma+2} - 2^{\gamma}3^{\gamma+3}) \\ & - a^42^{-4\gamma-5}3^{-2\gamma-3}5^{-\gamma-2}(2^{4\gamma+7}3^{2\gamma+3} - 2^{4\gamma+6}5^{\gamma+2} - 3^{2\gamma+3}5^{\gamma+2} + 2^{2\gamma+3}3^{\gamma+1}5^{\gamma+3} - 2^{\gamma}3^{2\gamma+3}5^{\gamma+3}) \\ & + O(a^5). \end{aligned} \quad (15)$$

The jump of the compressibility factor is expressed as (see Fig. 1):

$$\Delta Z(a) = Z|_{K=1} - Z|_{\text{Bose}} = \frac{a}{2^{\gamma+1}} + O(a^2), \quad (16)$$

while the jump of the *specific* energy  $E_{\text{spec}}$  is of the form

$$\Delta E_{\text{spec}}(a) = T(\gamma + 1)\Delta Z(a) = T(\gamma + 1)\frac{a}{2^{\gamma+1}} + O(a^2). \quad (17)$$

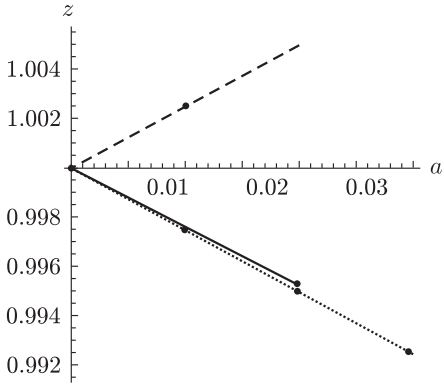


Figure 1: Dependence of the compressibility factor  $Z$  on the activity  $a$  for the two-dimensional case. Here  $\Phi = 100$ ,  $\gamma = 0$ . The upper (dashed) curve corresponds to the Fermi system. The middle (solid) curve corresponds to the Bose system up to  $O(a^2)$ . The lower (dotted) curve corresponds to the exact Bose system. The points on the curves correspond integer  $N$ .

The dependence of the compressibility factor  $Z$  on the activity  $a$  for the case  $\gamma = 0$  is shown in Fig. 1.

**4.** As indicated above, the author obtained a self-consistent equation in which  $N$  is an unknown quantity. We are interested in the point at which the number of Bose particles  $N$  is 0, i.e., the point at which Bose particles vanish. An example of this point is given in Fig. 2. Let us note that the value of the activity  $a$  is not zero at this point; it depends essentially on the function  $\Phi$  and the parameter  $\gamma$ . Let us consider successively the cases of small  $N$ ,  $\gamma \geq 0$ , and  $\gamma < 0$ .

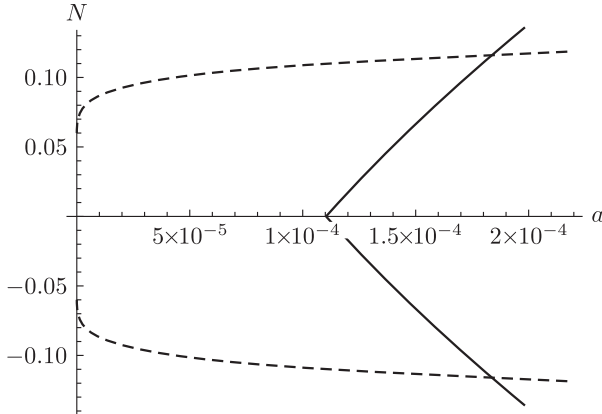


Figure 2: Dependence  $N(a)$  for  $W = 1000$ , where  $W = V(\lambda^2 T)^{\gamma+1}$ ,  $\lambda$  is the parameter depending on the mass, and  $\gamma = 0$ . The dotted curve corresponds to  $N = -1/\log(a)$ . The solid line corresponds to  $N = 0$ .

**4.1.** As pointed out above, there can be at most  $N$  particles at each energy level. Therefore, for the Bose system, we put  $k = N$ . Equation (8) takes the form:

$$N = \Phi(Li_{1+\gamma}(a) - \frac{1}{(N+1)^\gamma} Li_{1+\gamma}(a^{N+1})). \quad (18)$$

Expanding the right-hand side of Eq. (18) in the small parameter  $N \ll a$ , we obtain

$$\begin{aligned} N &= \Phi N (\gamma \text{Li}_{\gamma+1}(a) - \log(a) \text{Li}_\gamma(a)) \\ &+ \frac{1}{2} W N^2 (\log^2(a) (-\text{Li}_{\gamma-1}(a)) - \gamma ((\gamma+1) \text{Li}_{\gamma+1}(a) - 2 \log(a) \text{Li}_\gamma(a))) + o((\log a N)^2). \end{aligned} \quad (19)$$

*Remark 2.* We deal with two double limits. The first case is

$$\lim_{a \rightarrow 0} a \lim_{N \rightarrow 0} N.$$

In this case,  $N \ll a$ , and we obtain some value of  $a_0$  for which the number of Bose particles of the distribution  $N = 0$ .

In the second case,  $N$  is fixed and  $a \ll N$ . As a result, the Gentile parastatistical term vanishes.

If, in the expansion (18), we take into account the terms up to the second order of smallness inclusive, then we can obtain the equation for  $N$  whose solution is as follows:

$$N = 2 \frac{\gamma \Phi \text{Li}_{\gamma+1}(a) - \Phi \log(a) \text{Li}_\gamma(a) - 1}{\Phi (\log^2(a) \text{Li}_{\gamma-1}(a) + \gamma ((\gamma+1) \text{Li}_{\gamma+1}(a) - 2 \log(a) \text{Li}_\gamma(a)))}. \quad (20)$$

Equation (20) yields the following equation for  $a_0$  in the case  $N = 0$ :

$$\gamma \Phi \text{Li}_{\gamma+1}(a_0) - \Phi \log(a_0) \text{Li}_\gamma(a_0) - 1 = 0, \quad (21)$$

For small  $a_0$ , the following asymptotic formula holds:

$$\Phi = -\frac{1}{a_0 \ln a_0}, \quad (22)$$

or

$$\Phi = \frac{1}{a_0 \ln \Phi}. \quad (23)$$

We obtain

$$\Delta Z(a_0) = \frac{a_0}{2^{\gamma+1}} = -\frac{1}{2^{\gamma+1} \Phi \ln a_0}. \quad (24)$$

The maximal number of particles  $N_c$  in the system is at the caustic point  $a = 1$ . The value of  $N_c$  is given by

$$N_c = \Phi (Li_{1+\gamma}(1) - \frac{1}{(N_c + 1)^\gamma} Li_{1+\gamma}(1)). \quad (25)$$

We shall use the integral representation of the polylogarithm  $\text{Li}$ , obtaining

$$N_c = \Phi \beta \int_0^\infty \left( \frac{1}{\exp\{\varepsilon/T\} - 1} - \frac{N_c + 1}{\exp\{(N_c + 1)\varepsilon/T\} - 1} \right) d\varepsilon, \quad \beta = 1/T. \quad (26)$$

**4.2.** Consider the case  $D = 2$ . Let  $N = N_c$  be the solution of Eq. (26). We shall evaluate the integral in (26) (with the same integra) taken from  $\delta$  to  $\infty$  and then pass to the limit as

$\delta \rightarrow 0$ . After making the change  $\beta x = \xi$  in the first term and  $\beta(N_c + 1)x = \xi$  in the second term, where  $\beta = 1/T$ , we obtain

$$N_c = \Phi \int_{\delta\beta}^{\infty} \frac{d\xi}{e^\xi - 1} - \Phi \int_{\delta\beta(N_c+1)}^{\infty} \frac{d\xi}{e^\xi - 1} + O(\delta) = \Phi \int_{\delta\beta}^{\delta\beta(N_c+1)} \frac{d\xi}{e^\xi - 1} + O(\delta) \quad (27)$$

$$\sim \Phi \int_{\delta\beta}^{\delta\beta(N_c+1)} \frac{d\xi}{\xi} + O(\delta) = \Phi \{ \ln(\delta\beta(N_c + 1)) - \ln(\delta\beta) \} + O(\delta) = \Phi \ln(N_c + 1) + O(\delta). \quad (28)$$

In the three-dimensional case, this formula is of the form (4).

After passing to the limit as  $\delta \rightarrow 0$ , we obtain

$$N_c = \Phi \log(N_c + 1). \quad (29)$$

Multiplying the difference of the specific energies  $\Delta E_{\text{spec}}(a_0)$  by the number of particles defined by formula (25), we obtain the difference of the energies for the whole system of particles in the units of  $T$  in the case  $\gamma > 0$ :

$$\Delta E = \Delta E_{\text{spec}}(a_0) N_c = \frac{\gamma + 1}{2^{\gamma+1} \ln \Phi} Li_{1+\gamma}(1) \left( 1 - \frac{1}{(N_c + 1)^\gamma} \right) \quad (30)$$

and, in the case  $\gamma = 0$ , we have

$$\Delta E = \Delta E_{\text{spec}}(a_0) N_c = \frac{1}{2 \ln \Phi} \log(N_c + 1), \quad (31)$$

where  $N_c$  can be calculated from formula (25) (which contains  $\Phi$ ).

**4.3.** Let us pass to the case  $\gamma < \gamma_0 < 0$ , i.e.,  $D < D_0 < 2$ .

For the case in which  $\gamma < \gamma_0 < 0$ , the following lemma holds.

**Lemma 1.** *Consider the integral*

$$N = B \int_0^{\infty} \left( \frac{1}{e^{\beta x - \beta \mu} - 1} - \frac{k}{e^{k(\beta x - \beta \mu)} - 1} \right) x^\gamma dx, \quad (32)$$

where  $-1 < \gamma < \gamma_0 < 0$ , and  $B > 0$  and  $k > 0$  are constants.

Then

$$N = -\frac{B}{\beta^{\gamma+1}} c_{\beta\mu,\gamma} + \frac{Bk^{-\gamma}}{\beta^{\gamma+1}} c_{k\beta\mu,\gamma}, \quad (33)$$

where

$$c_{\mu,\gamma} = \int_0^{\infty} \left( \frac{1}{\xi - \mu} - \frac{1}{e^{\xi - \mu} - 1} \right) \xi^\gamma d\xi. \quad (34)$$

By the Lemma, Eq. (19) takes the form

$$N_c = \Phi C(\gamma) (-1 + (N_c + 1)^{-\gamma}), \quad (35)$$

where

$$C(\gamma) = \frac{1}{\Gamma(\gamma + 1)} \int_0^{\infty} \left( \frac{1}{\xi} - \frac{1}{e^\xi - 1} \right) \xi^\gamma d\xi. \quad (36)$$

As  $N_c \rightarrow \infty$ , we can neglect the summand  $-1$  in formula (35) as well as  $1$  compared to  $N_c$ , whence we obtain

$$N_c = \Phi C(\gamma) N_c^{-\gamma}, \quad (37)$$

$$N_c = (\Phi C(\gamma))^{1/(\gamma+1)} = T \left( \left( \frac{\sqrt{2\pi m}}{2\pi\hbar} \right)^{2(\gamma+1)} V C(\gamma) \right)^{1/(\gamma+1)}; \quad (38)$$

as a final result, we arrive at the expression

$$N_c = T (V C(\gamma))^{1/(\gamma+1)} \left( \frac{\sqrt{2\pi m}}{2\pi\hbar} \right)^2. \quad (39)$$

For the jump of the energy, we obtain the expression

$$\Delta E = \frac{\gamma+1}{2^{\gamma+1} \Phi \ln \Phi} (\Phi C(\gamma))^{1/(\gamma+1)} = \frac{\gamma+1}{2^{\gamma+1} \ln \Phi} C(\gamma)^{1/(\gamma+1)} \Phi^{-\gamma/(\gamma+1)}. \quad (40)$$

## 2 Using infinitesimal quantities to describe the separation process of neutrons from atomic nuclei

A Bose particle consists of two Fermi particles which are linked together by an interaction force or, as it is customary to say at the present time, by an entangling force. Sometimes the two fermions constituting the boson are absolutely identical. They cannot be distinguished or numbered. Sometimes the fermions differ in mass, then they can be distinguished. For example, a proton and an electron are fermions of different mass, and together they constitute a pair – a boson. Such fermions can be distinguished and numbered, using the mechanism of numeration theory. While if the masses of the particles approach each other and coincide in the limit, then we cannot distinguish them.

The passage from the case of distinguishable particles to the case when the particles become undistinguishable leads to other quantum-mechanical formulas and therefore, to different commutation relations [8].

The separation of a fermion from the nucleus and the capture of a fermion is a very rapid process. The question of the possibility of monitoring that transformation as if it occurred in slow motion arises. Mathematically, this means that we must use such tools which may be applied to both fermions and bosons.

In the present paper we use infinitely small quantities to modify the parastatistical distribution (the Gentile statistical method). This approach allows to apply the “antipod” of the P-Z chart corresponding to the Van-der-Waals equation of state in thermodynamics, also known as the Hougen–Watson chart. In this antipode, the isotherms under consideration, unlike those in the Van-der-Waals model, correspond to extremely high temperatures, which increase even more when the compressibility factor  $Z$  decreases.

The obtained antipode of the P-Z chart adequately corresponds to the behavior of nuclear matter. We will show in this paper that the passage of particles satisfying the Fermi–Dirac distribution to the Bose–Einstein distribution in the neighborhood of pressure  $P$  equal to zero occurs in a region known as the “halo”. This region is different for various isotopes and depends on chemical potentials.

The method developed in this paper differs from those in other models based on the interaction of two or three particles, such as the Faddeev–Skyrme model or models involving the Lennard–Jones potential. This method is based on interpolation formulas yielding

expansions in powers of the density. Just as in the Van-der-Waals interpolation formula, the zeroth approximation is given by ideal gas, whereas in models based on potentials the zeroth approximation is given by the zero potential.

Niels Bohr in 1936 proposed one of the earliest models of the atomic nucleus in the framework of the theory of compound nucleus [9]. Later, by Carl Weizsäcker was obtained a semi-empirical formula for the binding energy of the atomic nucleus  $E_c$ :

$$E_c = \alpha A - \beta A^{2/3} - \gamma \frac{\mathcal{Z}^2}{A^{1/3}} - \varepsilon \frac{(A/2 - \mathcal{Z})^2}{A} + \delta, \quad (41)$$

where

$$\delta = \begin{cases} + \chi A^{-3/4} & \text{for even-even nuclei,} \\ 0 & \text{for nuclei with odd } A, \\ - \chi A^{-3/4} & \text{for odd-odd nuclei,} \end{cases}$$

$A$  is the mass number (total number of nucleons) in the nucleus,  $\mathcal{Z}$  is the charge number (number of protons) in the nucleus, and  $\alpha$ ,  $\beta$ ,  $\gamma$ ,  $\varepsilon$ , and  $\chi$  are parameters obtained by statistical treatment of experimental data. This formula provides sufficiently exact values of the binding energies and masses for many nuclei, which permits using it to analyze different properties of the atomic nucleus.

In this paper we obtain new important relations between the temperature and the chemical potential in the process of nucleon separation from the atomic nucleus. For this, we use the parastatistic relations modified by the mathematical notion of infinitesimals.

## 2.1 New parastatistics

Let us assume that the energy of each of the particles takes one of the values of the given discrete spectrum. We shall denote by  $N_i$  the number of particles located at the  $i$ -th level energy.

Besides the Bose–Einstein and Fermi–Dirac statistics, physicists use parastatistics (aka Gentile statistics [6]) that generalizes the two previously mentioned statistics, which are thus particular cases of parastatistics. According to the latter, as it was said earlier, at each energy level, there may be no more than  $K$  particles. By the usual definitions, the Fermi case is realized for  $K = 1$ . In the case of Bose statistics  $N_i \leq N$  because then  $\sum_i N_i = N$ , implies that  $K = N$ .

We will be dealing with infinitely small  $K$  and  $N$  equal to each other. General approach see in [10].

In the case of parastatistics, we have the following relations, in which the first term in parentheses gives the distribution for Bose particles, and the second term, the parastatistical correction (compare (7)-(8)):

$$E = \frac{V}{\lambda^D} T(\gamma + 1) (\text{Li}_{2+\gamma}(a) - \frac{1}{(K+1)^{\gamma+1}} \text{Li}_{2+\gamma}(a^{K+1})), \quad (42)$$

$$N = \frac{V}{\lambda^D} (\text{Li}_{1+\gamma}(a) - \frac{1}{(K+1)^\gamma} \text{Li}_{1+\gamma}(a^{K+1})), \quad (43)$$

where  $\text{Li}_{(\cdot)}(\cdot)$  is the polylogarithm function,  $a = e^{\mu/T}$  is the activity ( $\mu$  being the chemical potential,  $T$  being the temperature),  $\gamma = D/2 - 1$ ,  $D$  is the number of degrees of freedom (the dimension),  $\lambda$  is the de Broglie wavelength:

$$\lambda = \sqrt{\frac{2\pi\hbar^2}{mT}}, \quad (44)$$

where  $\hbar$  is the Planck constant,  $m$  the mass of one particle.

The de Broglie wavelength is related to the Bohr–Sommerfeld quantization condition, i.e., to the quantization of the angular momentum (see [11] and related works, in particular [12]–[18]).

## 2.2 Passage from the Bose-type region to the Fermi-type region through a nuclear halo

Before completely separating from a nucleus, a nucleon stays within an area around a nucleus where it is bound to a nucleus with entanglement forces. In this area the probability to discover a neutron is higher than the probability to discover a proton. It is well-known that the area where the density distribution of neutrons much exceeds the density distribution of protons is called a nuclear halo.

The region corresponding to the difference of pressure  $P = 0$  and to an infinitely small sequence  $\{P_K\} \rightarrow 0$  constitutes the nuclear halo. The passage from the Bose-type region to the Fermi-type region occurs through the nuclear halo, which contains the value of the pressure  $P = 0$ . We denote by  $a_0$  the maximal value of the activity  $a$  for Bose particles as  $N \rightarrow 0$ . The quantity  $a_0$  indicates the maximal value of the activity at which the decomposition of bosons into fermion occurs.

Let us recall some definitions and relationships that we used in the paper [19]. It will be helpful to consider more general cases later in this work.

For an ideal gas of dimension  $D = 3$ , relations (42), (43) become

$$N = \frac{V}{\lambda^3} (\text{Li}_{3/2}(a) - \frac{1}{(K+1)^{1/2}} \text{Li}_{3/2}(a^{K+1})), \quad (45)$$

$$E = \frac{3}{2} \frac{V}{\lambda^3} T (\text{Li}_{5/2}(a) - \frac{1}{(K+1)^{3/2}} \text{Li}_{5/2}(a^{K+1})). \quad (46)$$

The expansion of the summand  $\frac{1}{(K+1)^{1/2}} \text{Li}_{3/2}(a^{K+1})$  from formula (45) in small values of  $K$  has the form:

$$\frac{1}{(K+1)^{1/2}} \text{Li}_{3/2}(a^{K+1}) = \text{Li}_{3/2}(a) - [K(\text{Li}_{3/2}(a)/2 - \log(a) \text{Li}_{1/2}(a)) + O(K^2)]. \quad (47)$$

Let  $B = V/\lambda^3 > 0$ . Then equation (45) for small  $K$  acquires the form:

$$N = BK(\frac{1}{2} \text{Li}_{3/2}(a) - \log(a) \text{Li}_{1/2}(a)) + O(K^2). \quad (48)$$

In our considerations  $N$  is an infinitely small number, ..  $N = \alpha_i$ , where a sequence of infinitesimals  $\alpha_i \rightarrow 0$  as  $i \rightarrow \infty$ . Similarly  $K = \beta_i$ , where a sequence of infinitesimals  $\beta_i \rightarrow 0$  as  $i \rightarrow \infty$ . The sequences  $\alpha_i$  and  $\beta_i$  are similar to each other, i.e.  $\lim_{i \rightarrow \infty} \frac{\alpha_i}{\beta_i} = 1$ . Thus we are not dealing with the Fermi statistics or the Bose statistics, but with a parastatistics of a new type, which can be called a Bose-like statistics.

Dividing both sides of (48) by  $N$  and taking the limit as  $K \rightarrow 0$ , yields an expression for  $a_0$ , i.e., the value of  $a$  for which  $K = N = 0$ :

$$\frac{1}{2} \text{Li}_{3/2}(a_0) - \log(a_0) \text{Li}_{1/2}(a_0) - B^{-1} = 0. \quad (49)$$

Equation (49) in the case of an arbitrary coefficient  $\gamma = D/2 - 1$  instead of  $1/2$ , after similar arguments, acquires the form:

$$\gamma \text{Li}_{\gamma+1}(a_0) - \log(a_0) \text{Li}_\gamma(a_0) - \frac{\lambda^{2(\gamma+1)}}{V} = 0. \quad (50)$$

Equation (50) has a unique solution  $a_0 > 0$  that depends on  $B$  and  $\gamma$ .

In the case  $K = N$ , equation (45) acquires the form

$$N = B(\text{Li}_{3/2}(a) - \frac{1}{(N+1)^{1/2}} \text{Li}_{3/2}(a^{N+1})). \quad (51)$$

This equation obviously has the solution  $N \equiv 0$  for any  $a \geq 0$ . However, for  $a > a_0$ , it has one more nonnegative solution  $N(a)$ . This can be verified by constructing the graphs of the right-hand and left-hand sides of (51) as a function of  $a$  for an arbitrary fixed  $N > 0$ . The right-hand side of the equation is zero for  $a = 0$  and monotonically grows for  $a \in (0, \infty)$ , while the left hand side is a constant that does not depend on  $a$ .

Substituting the obtained relation  $N(a)$  in formula (46), we can find the dependence  $E(a)$ , and with it the pressure  $P(a)$ , by using the relation

$$E = (\vec{\gamma} + 1)PV. \quad (52)$$

Let us substitute the obtained relation into the graph of the compressibility factor

$$Z = PV/(NT) \quad (53)$$

as a function of  $P$  (this graph is known as the Hougen–Watson chart).

Now we place a minus sign before dependencies  $P(a)$  and  $N(a)$  for the Bose branch, i.e. these values are considered as negative. It follows from this that in the Bose-like region  $Z(a) > 0$ .

The value  $a = a_0$  is the minimum value of activity for the Bose branch, since for  $a < a_0$  the region of uncertainty occurs where  $N \equiv 0$  and  $P \equiv 0$  for all  $a$  up to the value of  $a = 0$ . Here the passage of particles to the Fermi branch begins.

For Fermi statistics in the case  $D = 3$ , we have the relations

$$N = -\frac{V}{\lambda^3} \text{Li}_{3/2}(-a), \quad (54)$$

$$E = -\frac{3}{2} \frac{V}{\lambda^3} T \text{Li}_{5/2}(-a). \quad (55)$$

Let us call the curve on the P-Z chart, constructed according to formulas (54)–(55) of Fermi statistics, the Fermi branch. The pressure  $P$ , as well as the number of particles  $N$ , on the Fermi branch is positive.

## 2.3 Construction of the isotherm for nuclear matter

The value of the activity  $a$  for a known value of the temperature  $T$  determines the corresponding value of the chemical potential

$$\mu = T \log(a). \quad (56)$$

In particular, for  $a = a_0$ , the higher the temperature, the smaller is  $a_0$ , and the larger is the value of  $|\mu_0|$ . Thus, as the temperature grows, the point of passage  $\mu_0$  approaches the point  $\mu = -\infty$  at which the pressure  $P$  changes sign (see [20]).

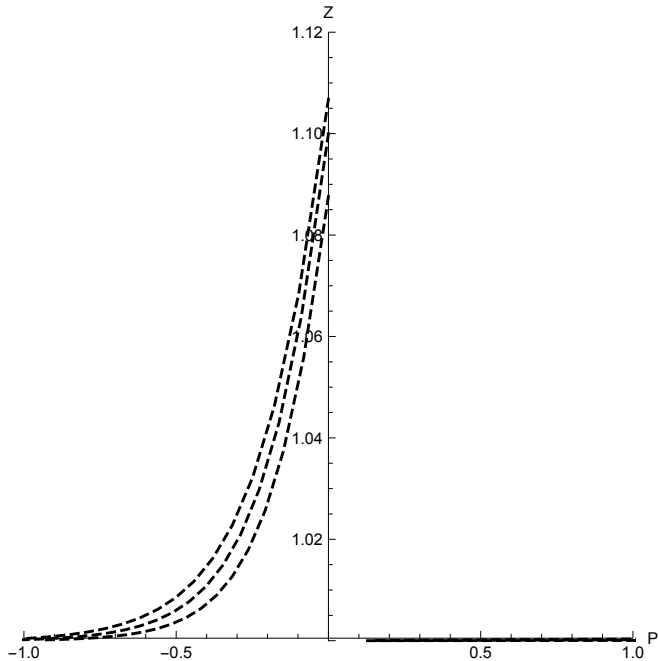


Figure 3: Dependence of the compressibility factor  $Z$  on the pressure  $P$ , expressed in the units  $\text{MeV}/\text{fm}^3$  for carbon-12, nitrogen-14, fluorine-19 (from top to bottom). The continuous line represents the line  $Z = 1$ . It is the beginning of the Fermi branch. The hashed lines show isotherms of the Bose branch, constructed according to formulas (45)–(46). The temperature is equal to the nucleus binding energy  $E_b$ . The corresponding values of  $E_b$  and  $a_0$  are given in Table 1 in Appendix.

Table 1 in Appendix presents values of  $a_0$  and  $\mu_0 = T \log a_0$  for isotopes of stable chemical elements.

The value of  $a_0$  in the case of separation can be found by means of formula (49), taking into account the expression of the de Broglie wavelength  $\lambda$  in terms of the volume  $V$  of the nucleus, its temperature  $T$  and its mass  $m$ . The volume of the nucleus is taken to be that of a ball of radius  $r_0 = A^{1/3}1.2 \times 10^{-15} \text{ m}^3$ . The temperature  $T$  of the nucleus expressed in energy units is taken equal to the binding energy of the nucleus  $E_b$ , equal to the core temperature  $T$  (obtained from the database IsotopeData).

Table 1 demonstrates a monotonic relation between the nucleus mass number  $A$ , the binding energy  $E_b$ , the minimum value of activity  $a = a_0$ , the chemical potential  $\mu_0 = T \log a_0$ , and the compressibility factor  $Z = PV/NT$  for  $a_0$ .

We have obtained an equation (49) from which we can find the value of  $a_0$ , and can determine the temperature  $T$  at which this value is attained.

Fig. 3 shows the dependence of the compressibility factor  $Z = PV/(NT)$  on the pressure  $P$ , expressed in the units  $\text{MeV}/\text{fm}^3$  carbon-12, nitrogen-14, fluorine-19. The dashed lines are the isotherms of the Bose branch constructed by means of formulas (45), (46), (53), and (52). The isotherms are parametric curves  $P(a)$ ,  $Z(a)$ .

Let  $\{P_K\}$  be an infinitely small sequence, coinciding with the infinitely small quantity  $K$ . It can be shown that the corresponding sequence  $\{Z_k\}$  tends to a number greater than unity in the Bose-like region and to unity in the Fermi-like region (see Fig. 3).

The temperature is equal to the extremal value of the binding energy  $E_b$ , indicated in Table 1. To each value of  $a_0$  there corresponds a definite value of the temperature  $T$ . In turn, to each value of  $T$  there corresponds an isotherm on the Hougen–Watson chart.

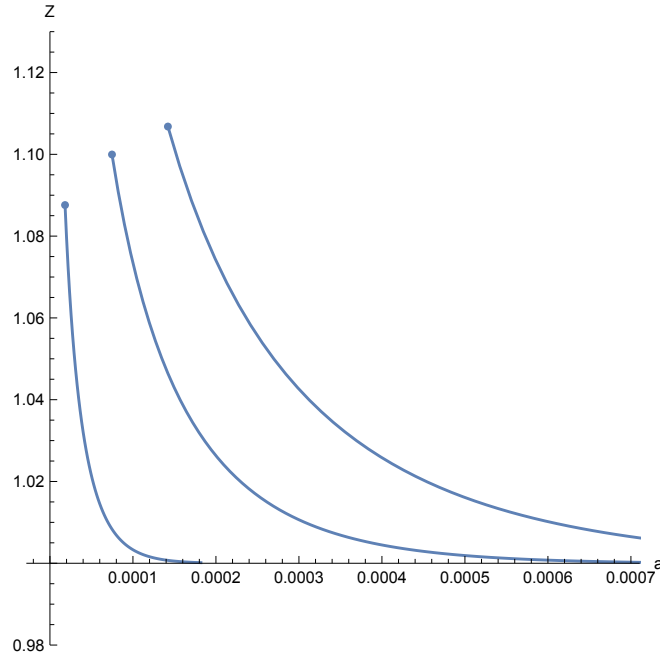


Figure 4: Dependence of the compressibility factor  $Z$  on the activity  $a$ , expressed in the units  $\text{MeV}/\text{fm}^3$  for fluorine-19, nitrogen-14, carbon-12 (from left to right). The lines show isotherms of the Bose branch, constructed according to formulas (45)–(46). The temperature is equal to the nucleus binding energy  $E_b$  (see Table 1 in Appendix).

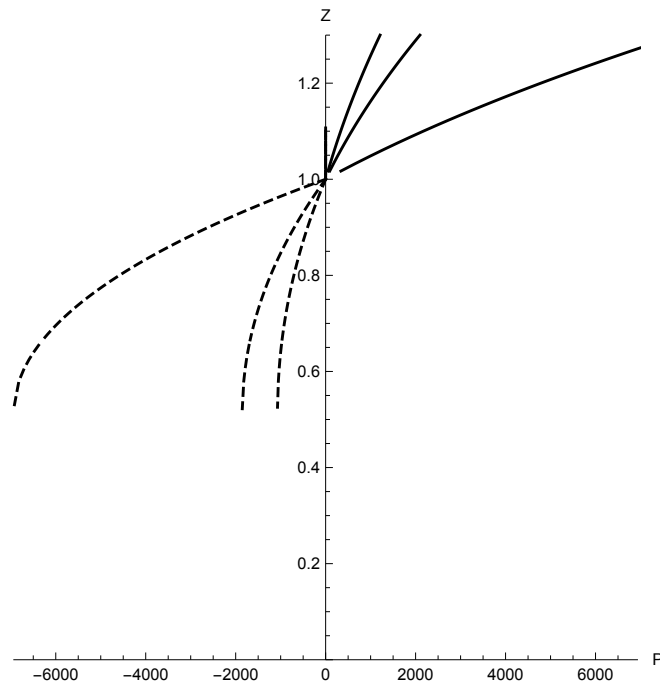


Figure 5: Dependence of the compressibility factor  $Z$  on the pressure  $P$ , expressed in the units  $\text{MeV}/\text{fm}^3$  for fluorine-19, nitrogen-14, carbon-12 (from left to right in the region  $P < 0$ ). The continuous line represents the Fermi branch. The hashed lines show isotherms of the Bose branch, constructed according to formulas (45)–(46).

These isotherms lie in the second quadrant. If the volume is constant, the temperature characterizing the isotherm becomes smaller as the point  $a = a_0$  becomes nearer to  $a = 1$ .

Thus we can say that the Van-der-Waals isotherms are in a sense opposite to the isotherms of nuclear matter shown in Fig. 3.

This shows that the chemical potential  $\mu$  at  $P = 0$  does not become equal to minus infinity and so the axis  $Z$  at  $P = 0$  is not the boundary between two unrelated structures. Since the value of  $|\mu_0|$  is very large but not infinite between the values of the infinitely small quantities  $\{P_K\}$  and the region obeying the Fermi-Dirac distribution, there is a “halo” dividing the Bose region from the Fermi region.

The value of the chemical potential  $\mu_0$  determines the halo width. The halo expands as  $\mu_0$  is close to zero. It can become infinitely large.

In the classical thermodynamics this situation corresponds to passing through the point where the pressure vanishes (i.e. passing from a negative compressibility factor  $Z$  to a positive  $Z$ ). The halo is a domain of indeterminacy: nobody knows what happens with the particles in the domain of a nuclear halo. We can refer to halo as the lacunary indeterminacy.

We do not consider the problem of proving that the isotherms on Fig. 3 exist. We give an approximate solution of the obtained equations (see similar approaches in papers [21], [22]), in which all the isotherms corresponding to different values of  $a_0$  are approximately constructed.

In the point  $a = 1$  (i.e. on the spinodal) the compressibility factor has the form:

$$Z_s = \frac{\zeta(5/2)}{\zeta(3/2)} \frac{1 - \frac{1}{(N_s+1)^{3/2}}}{1 - \frac{1}{(N_s+1)^{1/2}}}, \quad (57)$$

where  $N_s$  is determined from the relation

$$N_s = \frac{V}{\lambda^3} \zeta(3/2) \left( 1 - \frac{1}{(N_s + 1)^{1/2}} \right). \quad (58)$$

In the Fig. 4 upper ends of isotherms correspond to  $a = a_0$ . In the Fig. 3 corresponding points lie on the axis  $Z$ . This makes it possible to consider and compare behavior of isotherms of different chemical elements.

In Fig. 5 isotherms shown in Fig. 3 are drawn on a different scale.

One can see in Fig. 5 that the tangent to the lead curve in the bend point is parallel to the axis  $Z$ . This is a very important point where the activity  $a = 1$ . It connects the matter under consideration with the Van-der-Waals gas. This point is evidence of passing to the nuclear matter. Nuclear matter is a substance which in contrast to the nucleus has no boundaries. The bending down of the lead isotherm indicates that in the separation process of neutrons from an atomic nuclei we pass to another substance of nuclear matter.

Thus we have described a complete picture of passing from a substance which occurs when a neutron separates from an atomic nucleus to the nuclear matter substance.

## Conclusion

We have shown that using infinitesimals  $N$  and  $K$  equally fast tending to zero leads to the determination of the value of a parameter  $a_0$  that allows us to construct an antipode of sorts of the Hougen-Watson P-Z chart for nuclear matter. We have shown that, knowing the values of  $a_0$ , we can construct all the isotherms on the P-Z chart. The smaller the value of  $a_0$  the higher temperature of nuclear matter is.

In the paper it was shown that during separation of neutrons from atomic nuclei, between Bose-like and Fermi-like regions there exists a nuclear halo related to the chemical potential

$\mu$ . The properties of halo may be used to model a medium for filtering radioactive elements. Such a filter turned out to be more efficient than the Darcy filtering medium used in the paper [23] (also see [24]).

The obtained in the paper rigorous mathematical approach unexpectedly yields a new picture, which adequately describes the passing to the nuclear matter during separation process of neutrons from atomic nuclei. This led to a new table for nuclear physics (see Appendix) which demonstrates a monotonic relation between the nucleus mass number  $A$ , the binding energy  $E_b$ , the minimum value of activity  $a = a_0$ , the chemical potential  $\mu_0 = T \log a_0$ , and the compressibility factor  $Z = PV/NT$  for  $a_0$ .

## References

- [1] G. V. Koval' and V. P. Maslov, "Ultrasecond quantization at temperatures distinct from zero," *Math. Notes* **82** (1) 52–57 (2007).
- [2] G. V. Koval' and V. P. Maslov, "Generalization of the Bardeen–Cooper–Schrieffer method for pair interactions," *Teoret. Mat. Fiz.* **154** (3) 495–502 (2008).
- [3] L. D. Landau and E. M. Lifshits, *Statistical Physics* (Fizmatlit, Moscow, 2013).
- [4] V. P. Maslov, *Perturbation Theory and Asymptotical Methods* (Izd. Moskov. Univ., Moscow, 1965; Dunod, Paris, 1972) [in Russian and French].
- [5] A. I. Shtern, "Remark concerning Maslov's theorem on homomorphisms of topological groups," *Russian J. Math. Phys.* **24** (2), 262–262 (2017).
- [6] W.-S. Dai and M. Xie, "Gentile statistics with a large maximum occupation number," *Ann. Phys.* **309**, 295–305 (2004).
- [7] I. A. Kvasnikov, *Thermodynamics and Statistical Physics: Theory of Equilibrium Systems* (URSS, Moscow, 2002), Vol. 2 [in Russian].
- [8] Salo, P. & Hietarinta, J. Ground state in the Faddeev-Skyrme model *Physical review D* **62** 081701(2000).
- [9] Bohr, N. Neutron capture and nucleus structure *Uspekhi Fiz. Nauk* **14** (4), 425–435 (1936).
- [10] Davis, M. & Hersh, R. Nonsstandard analysis *Scientific American* 226 (6), 78–86 (1972).
- [11] Litvinov, G. L. The Maslov dequantization, idempotent and tropical mathematics: a very brief introduction. *Contemp. Math.*, Vol. 377: *Idempotent Mathematics and Mathematical Physics* (Amer. Math. Soc., Providence, RI, 2005).
- [12] Tyurin, N.A. Universal Maslov class of a Bohr-Sommerfeld Lagrangian embedding into a pseudo-Einstein manifold. *Theoretical and Mathematical Physics* **150** (2), 278–287 (2007).
- [13] Yoshioka, A. Maslov's Quantization Conditions for the Bound States of the Hydrogen Atom. *Tokyo J. Math.* **09** (2), 415–437 (1986).
- [14] Czyż, J. On geometric quantization and its connection with the Maslov theory. *Reports of Math. Physics* **15** (1), 57–97 (1979).

- [15] Barilari, D. & Lerario, A. Geometry of Maslov cycles. *Geometric Control Theory and Sub-Riemannian Geometry*. Springer INdAM Series, v.5, 15-35 — (Springer, 2014).
- [16] Borrelli, V. Maslov form and J-volume of totally real immersions. *J. Geom. Phys.* **25** (3-4), 271–290 (1998).
- [17] Littlejohn, R.G. Cyclic evolution in quantum mechanics and the phases of Bohr-Sommerfeld and Maslov. *Phys Rev Lett.* **61**(19), 2159–2162 (1988).
- [18] Chen, B. Y. Maslovian Lagrangian surfaces of constant curvature in complex projective or complex hyperbolic planes *Mathematische Nachrichten* **278** (11), 1242–1281 (2005).
- [19] Maslov, V. P. Thermodynamic Concept of Neutron Separation Energy <https://arxiv.org/abs/1812.02586v4> [physics.gen-ph] (2018).
- [20] Maslov, V. P. Case of less than two degrees of freedom, negative pressure, and the Fermi–Dirac distribution for a hard liquid. *Math. Notes* **98** (1) 138–157 (2015).
- [21] Bruno, A. D. Self-similar solutions and power geometry *Russian Mathematical Surveys* **55** (1), 1–42 (2000).
- [22] Weinstein, A. The Maslov Gerbe *Letters in Mathematical Physics* **69** (1), 3–9 (2004).
- [23] Maslov, V. P., Myasnikov, V. P. & Danilov V. G. *Mathematical Modeling of the Accident Block of Chernobyl Atomic Station* (Nauka, Moscow, 1987) [in Russian].
- [24] Maslov, V. P. On mathematical investigations related to the Chernobyl disaster. *Russian J. Math. Phys.* **25** (3), 309–318 (2018).
- [25] Maslov, V. P. Statistics corresponding to classical thermodynamics. Construction of isotherms, *Russian J. Math. Phys.*, **22** (1), 53–67 (2015).
- [26] Maslov, V. P. Locally ideal liquid *Russian J. Math. Phys.* **22** (3), 361–373 (2015).

## Additional information

**Competing interests:** The author declares no competing interests.

# Appendix

Table 1 is based on the IsotopeData which contains 256 stable elements. The table does not include 2 elements: hydrogen-1 and lithium-3.

Table 1: Parameters for stable isotopes of various nuclei

	nucleus	$E_b$ , MeV	$a_0$	$\mu_0$ , MeV	$Z(a_0)$
1	lead-208	1636.430	6.56723452042905*^-10	-34600.3	1.0462
2	lead-207	1629.062	6.698086767960848*^-10	-34412.4	1.04624
3	lead-206	1622.324	6.828015748192335*^-10	-34238.9	1.04629
4	thallium-205	1615.071	6.964588838317156*^-10	-34053.8	1.04633
5	mercury-204	1608.651	7.098772812928244*^-10	-33887.7	1.04637
6	lead-204	1607.506	7.10672952303982*^-10	-33861.8	1.04637
7	thallium-203	1600.869	7.245880420961687*^-10	-33690.9	1.04641
8	mercury-202	1595.164	7.381635822897305*^-10	-33541.3	1.04645
9	mercury-201	1587.410	7.535854034104263*^-10	-33345.4	1.0465
10	mercury-200	1581.180	7.682432530030704*^-10	-33184.1	1.04654
11	mercury-199	1573.152	7.846660093726309*^-10	-32982.3	1.04659
12	platinum-198	1567.005	8.000123077567905*^-10	-32823.1	1.04663
13	mercury-198	1566.487	8.004285468835854*^-10	-32811.4	1.04663
14	gold-197	1559.385	8.169474611920787*^-10	-32630.8	1.04667
15	platinum-196	1553.603	8.327773443812714*^-10	-32480.	1.04672
16	mercury-196	1551.217	8.347933880193217*^-10	-32426.4	1.04672
17	platinum-195	1545.681	8.508410497880471*^-10	-32281.2	1.04676
18	platinum-194	1539.576	8.677791457511231*^-10	-32123.4	1.04681
19	iridium-193	1532.057	8.86424234999922*^-10	-31933.9	1.04685
20	osmium-192	1526.115	9.040975977576068*^-10	-31779.9	1.0469
21	platinum-192	1524.963	9.051730687800583*^-10	-31754.1	1.0469
22	iridium-191	1518.087	9.242065249263186*^-10	-31579.4	1.04694
23	osmium-190	1512.798	9.421823243037092*^-10	-31440.2	1.04699
24	osmium-189	1505.006	9.631128432048317*^-10	-31245.2	1.04703
25	osmium-188	1499.09	9.82688720596613*^-10	-31092.1	1.04708
26	osmium-187	1491.096	1.0049538919691788*^-9	-30893.	1.04713
27	tungsten-186	1485.881	1.0248286832318242*^-9	-30755.9	1.04717
28	rhenium-185	1478.340	1.0477870466992142*^-9	-30567.	1.04722
29	tungsten-184	1472.936	1.068940371324127*^-9	-30425.8	1.04727
30	osmium-184	1469.920	1.0723954688763233*^-9	-30358.8	1.04727
31	tungsten-183	1465.52	1.0929829488547705*^-9	-30240.2	1.04732
32	tungsten-182	1459.334	1.1162283650585708*^-9	-30081.7	1.04736
33	tantalum-181	1452.239	1.141209677721084*^-9	-29903.3	1.04741
34	hafnium-180	1446.297	1.1654244706590216*^-9	-29750.6	1.04746
35	tungsten-180	1444.588	1.1675960361483143*^-9	-29712.7	1.04746
36	hafnium-179	1438.909	1.1921663900543855*^-9	-29566.	1.04751
37	hafnium-178	1432.810	1.2179463852540806*^-9	-29410.	1.04756
38	hafnium-177	1425.184	1.2465244369799248*^-9	-29220.4	1.04761
39	ytterbium-176	1419.3	1.2734992136223842*^-9	-29069.	1.04766
40	hafnium-176	1418.800	1.2741795612629933*^-9	-29058.4	1.04766
41	lutetium-175	1412.105	1.303055655692589*^-9	-28889.6	1.04771
42	ytterbium-174	1406.594	1.3309799436747485*^-9	-28747.1	1.04776

	nucleus	$E_b$ , MeV	$a_0$	$\mu_0$ , MeV	$Z(a_0)$
43	ytterbium-173	1399.130	1.3626480007147378*^-9	-28561.6	1.04782
44	ytterbium-172	1392.763	1.3935250264537363*^-9	-28400.4	1.04787
45	ytterbium-171	1384.743	1.4279570122720166*^-9	-28203.1	1.04792
46	erbium-170	1379.039	1.4595811641167073*^-9	-28056.7	1.04797
47	ytterbium-170	1378.129	1.4611005634016678*^-9	-28036.8	1.04798
48	thulium-169	1371.351	1.4954862724997947*^-9	-27867.	1.04803
49	erbium-168	1365.779	1.5287537012274288*^-9	-27723.7	1.04808
50	ytterbium-168	1362.792	1.5340368276133707*^-9	-27658.4	1.04809
51	erbium-167	1358.007	1.5669400332028521*^-9	-27532.4	1.04814
52	erbium-166	1351.571	1.6038170428593423*^-9	-27370.5	1.04819
53	holmium-165	1344.255	1.6434726602586052*^-9	-27189.5	1.04825
54	dysprosium-164	1338.034	1.6821790000731178*^-9	-27032.5	1.0483
55	erbium-164	1336.446	1.6853311429280429*^-9	-26998.	1.04831
56	dysprosium-163	1330.376	1.724960214068269*^-9	-26844.4	1.04836
57	dysprosium-162	1324.11	1.7661791350126498*^-9	-26686.6	1.04842
58	erbium-162	1320.696	1.7733706996456026*^-9	-26612.5	1.04843
59	dysprosium-161	1315.908	1.81280537192023*^-9	-26487.1	1.04848
60	dysprosium-160	1309.454	1.8570654316088657*^-9	-26325.6	1.04853
61	gadolinium-160	1309.289	1.8574339528585125*^-9	-26322.	1.04853
62	terbium-159	1302.026	1.9049205615658426*^-9	-26143.2	1.04859
63	gadolinium-158	1295.895	1.9512327020853415*^-9	-25988.9	1.04865
64	dysprosium-158	1294.05	1.9556313514825366*^-9	-25948.9	1.04866
65	gadolinium-157	1287.96	2.0033764311313157*^-9	-25795.8	1.04871
66	gadolinium-156	1281.597	2.053268321955851*^-9	-25636.9	1.04877
67	dysprosium-156	1278.020	2.0623376828811236*^-9	-25559.7	1.04878
68	gadolinium-155	1273.061	2.110392182825751*^-9	-25431.2	1.04884
69	samarium-154	1266.939	2.162984112868796*^-9	-25277.7	1.0489
70	gadolinium-154	1266.626	2.163827364719629*^-9	-25270.9	1.0489
71	europium-153	1259.00	2.222273587810274*^-9	-25085.2	1.04896
72	samarium-152	1253.104	2.277708227113307*^-9	-24936.9	1.04902
73	europium-151	1244.140	2.343969975869246*^-9	-24722.8	1.04909
74	samarium-150	1239.249	2.400144134332091*^-9	-24596.3	1.04915
75	samarium-149	1231.263	2.4677736023385272*^-9	-24403.6	1.04921
76	neodymium-148	1225.028	2.5320600244177075*^-9	-24248.5	1.04928
77	neodymium-146	1212.403	2.6675438118407026*^-9	-23935.4	1.0494
78	neodymium-145	1204.837	2.7431621345729796*^-9	-23752.3	1.04947
79	samarium-144	1195.736	2.8271802932673597*^-9	-23536.9	1.04954
80	neodymium-143	1191.265	2.8965569154578765*^-9	-23420.	1.0496
81	cerium-142	1185.289	2.9740366249990177*^-9	-23271.2	1.04967
82	neodymium-142	1185.141	2.9746227149814658*^-9	-23268.1	1.04967
83	praseodymium-141	1177.918	3.059829371144494*^-9	-23093.	1.04974
84	cerium-140	1172.692	3.1396291883311703*^-9	-22960.3	1.0498
85	lanthanum-139	1164.551	3.2347877245164052*^-9	-22766.2	1.04988
86	barium-138	1158.29	3.3250018143016076*^-9	-22611.9	1.04995
87	cerium-138	1156.034	3.335260696578726*^-9	-22564.3	1.04995
88	barium-137	1149.680	3.429421364336115*^-9	-22408.3	1.05002
89	barium-136	1142.775	3.5296016566547925*^-9	-22240.8	1.05009
90	xenon-136	1141.877	3.53398193939942*^-9	-22221.9	1.0501

	nucleus	$E_b$ , MeV	$a_0$	$\mu_0$ , MeV	$Z(a_0)$
91	cerium-136	1138.791	3.549117109921999*^-9	-22157.	1.05011
92	barium-135	1133.667	3.644595122640692*^-9	-22027.2	1.05018
93	xenon-134	1127.434	3.749122919718309*^-9	-21874.2	1.05025
94	barium-134	1126.695	3.7530095524334995*^-9	-21858.7	1.05025
95	cesium-133	1118.527	3.871987465425949*^-9	-21665.3	1.05033
96	xenon-132	1112.448	3.983836776114648*^-9	-21515.9	1.0504
97	barium-132	1110.037	3.997509802560838*^-9	-21465.4	1.05041
98	xenon-131	1103.511	4.1165194993787506*^-9	-21306.9	1.05048
99	xenon-130	1096.91	4.240446453994573*^-9	-21146.8	1.05056
100	barium-130	1092.721	4.266132000876623*^-9	-21059.5	1.05058
101	xenon-129	1087.7	4.385881720220346*^-9	-20931.7	1.05065
102	xenon-128	1080.742	4.521995791942188*^-9	-20765.7	1.05072
103	iodine-127	1072.576	4.672036852075847*^-9	-20573.8	1.05081
104	tellurium-126	1066.368	4.814295823368357*^-9	-20422.7	1.05089
105	xenon-126	1063.908	4.831906177465934*^-9	-20371.7	1.0509
106	tellurium-125	1057.255	4.983561714197291*^-9	-20211.7	1.05098
107	tellurium-124	1050.686	5.1405308687317735*^-9	-20053.5	1.05106
108	tin-124	1049.963	5.146128596004507*^-9	-20038.6	1.05106
109	xenon-124	1046.257	5.174972111525734*^-9	-19962.	1.05107
110	antimony-123	1042.096	5.319958844052601*^-9	-19853.8	1.05115
111	tin-122	1035.529	5.490224671390237*^-9	-19696.1	1.05123
112	tellurium-122	1034.333	5.500269600522192*^-9	-19671.4	1.05123
113	antimony-121	1026.325	5.690362777390483*^-9	-19484.3	1.05132
114	tin-120	1020.546	5.868347121824327*^-9	-19343.1	1.0514
115	tellurium-120	1017.281	5.898159918055959*^-9	-19276.1	1.05142
116	tin-119	1011.438	6.084867107538478*^-9	-19133.8	1.0515
117	tin-118	1004.954	6.285334777769982*^-9	-18978.6	1.05159
118	tin-117	995.627	6.52344834889344*^-9	-18765.4	1.05169
119	tin-116	988.6835	6.747033495964996*^-9	-18601.3	1.05178
120	tin-115	979.1201	7.0097924447818895*^-9	-18383.9	1.05188
121	cadmium-114	972.5984	7.249349259373691*^-9	-18228.8	1.05197
122	tin-114	971.5737	7.261450849502032*^-9	-18208.	1.05197
123	indium-113	963.0935	7.535962778087417*^-9	-18013.3	1.05207
124	cadmium-112	957.015	7.792405092235586*^-9	-17867.6	1.05216
125	tin-112	953.5315	7.837509842761975*^-9	-17797.	1.05218
126	cadmium-111	947.6211	8.104495048118805*^-9	-17655.	1.05227
127	cadmium-110	940.645	8.397948660268989*^-9	-17491.6	1.05237
128	palladium-110	940.2061	8.404157992997987*^-9	-17482.7	1.05237
129	silver-109	931.7259	8.73347567542745*^-9	-17289.2	1.05248
130	palladium-108	925.2386	9.048002150779387*^-9	-17136.1	1.05257
131	cadmium-108	923.4019	9.076511523777559*^-9	-17099.2	1.05258
132	silver-107	915.2624	9.43340089401213*^-9	-16913.1	1.05269
133	palladium-106	909.4742	9.767729345541411*^-9	-16774.5	1.05279
134	cadmium-106	905.1395	9.8419094237758*^-9	-16687.7	1.05281
135	palladium-105	899.9132	1.0184224243741393*^-8	-16560.6	1.0529
136	ruthenium-104	893.0826	1.0571578456048812*^-8	-16401.5	1.05301
137	palladium-104	892.8191	1.0576521551130673*^-8	-16396.3	1.05301
138	rhodium-103	884.16	1.1018537348225694*^-8	-16201.1	1.05312

	nucleus	$E_b$ , MeV	$a_0$	$\mu_0$ , MeV	$Z(a_0)$
139	ruthenium-102	877.9491	1.1433086860699268*^-8	-16054.8	1.05323
140	palladium-102	875.2115	1.1489797304816046*^-8	-16000.4	1.05324
141	ruthenium-101	868.7295	1.1932374944436193*^-8	-15849.1	1.05335
142	ruthenium-100	861.9274	1.2403651641649362*^-8	-15691.6	1.05346
143	ruthenium-99	852.2541	1.2967219219333479*^-8	-15477.7	1.05359
144	molybdenum-98	846.2422	1.3469994938753383*^-8	-15336.3	1.0537
145	ruthenium-98	844.7903	1.3506711074018759*^-8	-15307.7	1.05371
146	molybdenum-97	837.5997	1.4067056237850838*^-8	-15143.3	1.05382
147	molybdenum-96	830.7783	1.4646221546070764*^-8	-14986.5	1.05394
148	ruthenium-96	826.4953	1.4766745501517917*^-8	-14902.4	1.05396
149	molybdenum-95	821.6240	1.5324059770452706*^-8	-14784.2	1.05407
150	zirconium-94	814.6768	1.5972358788308048*^-8	-14625.4	1.05419
151	molybdenum-94	814.2550	1.598548223640437*^-8	-14617.2	1.0542
152	niobium-93	805.7646	1.6719544291673145*^-8	-14428.6	1.05433
153	zirconium-92	799.7212	1.7411000774507173*^-8	-14288.	1.05445
154	molybdenum-92	796.5077	1.7522569763461718*^-8	-14225.4	1.05447
155	zirconium-91	791.0864	1.823282061774853*^-8	-14097.2	1.05459
156	zirconium-90	783.892	1.9047600801369214*^-8	-13934.7	1.05472
157	yttrium-89	775.5375	1.9955349832973184*^-8	-13750.1	1.05486
158	strontium-88	768.4684	2.086183018013158*^-8	-13590.6	1.05499
159	strontium-87	757.3557	2.200525249737206*^-8	-13353.7	1.05515
160	krypton-86	749.2343	2.3080538147171625*^-8	-13174.7	1.0553
161	strontium-86	748.9276	2.3095546546447184*^-8	-13168.9	1.0553
162	rubidium-85	739.2825	2.4317040210891604*^-8	-12961.2	1.05546
163	krypton-84	732.2571	2.547423484973919*^-8	-12804.	1.0556
164	strontium-84	728.9053	2.5660547376695088*^-8	-12740.	1.05562
165	krypton-83	721.7365	2.6906313744512626*^-8	-12580.5	1.05577
166	krypton-82	714.2731	2.8246549743242437*^-8	-12415.7	1.05592
167	bromine-81	704.3694	2.98341213448522*^-8	-12205.	1.05609
168	selenium-80	696.8655	3.136144027103749*^-8	-12040.2	1.05625
169	krypton-80	695.4334	3.146415488574621*^-8	-12013.2	1.05626
170	bromine-79	686.32	3.321963170171236*^-8	-11818.5	1.05643
171	selenium-78	679.9890	3.487013115049057*^-8	-11676.5	1.05659
172	krypton-78	675.5780	3.523283574672109*^-8	-11593.8	1.05662
173	selenium-77	669.4912	3.6987047053968185*^-8	-11456.8	1.05678
174	selenium-76	662.0723	3.8975796000438735*^-8	-11295.2	1.05695
175	arsenic-75	652.564	4.130850959421723*^-8	-11095.	1.05714
176	germanium-74	645.66	4.35353384481982*^-8	-10943.8	1.05731
177	selenium-74	642.8904	4.383467178372254*^-8	-10892.4	1.05733
178	germanium-73	635.4686	4.6292952227919157*^-8	-10732.	1.05751
179	germanium-72	628.6856	4.884545815217069*^-8	-10583.7	1.05769
180	gallium-71	618.951	5.196732828530435*^-8	-10381.4	1.05789
181	zinc-70	611.0864	5.507095313502531*^-8	-10214.1	1.05809
182	germanium-70	610.5202	5.5152314411545844*^-8	-10203.7	1.0581
183	gallium-69	601.9959	5.8597253632622124*^-8	-10024.8	1.0583
184	zinc-68	595.3864	6.199386123424248*^-8	-9881.17	1.05849
185	zinc-67	585.1883	6.6281283373498*^-8	-9672.79	1.05872
186	zinc-66	578.1360	7.032839153071006*^-8	-9521.95	1.05893

	nucleus	$E_b$ , MeV	$a_0$	$\mu_0$ , MeV	$Z(a_0)$
187	copper-65	569.2112	7.507890564581662*^-8	-9337.75	1.05916
188	nickel-64	561.7579	7.989860837290716*^-8	-9180.53	1.05937
189	zinc-64	559.0975	8.050575715399685*^-8	-9132.82	1.0594
190	copper-63	551.3844	8.58281334385522*^-8	-8971.53	1.05963
191	nickel-62	545.2620	9.116779113755632*^-8	-8839.01	1.05984
192	nickel-61	534.6655	9.822516585416794*^-8	-8627.37	1.06011
193	nickel-60	526.8454	1.0508317053214359*^-7	-8465.62	1.06036
194	cobalt-59	517.3128	1.1314022740258889*^-7	-8274.23	1.06063
195	iron-58	509.9488	1.2114949455850543*^-7	-8121.57	1.06088
196	nickel-58	506.4584	1.2248587106385168*^-7	-8060.42	1.06092
197	iron-57	499.9042	1.309886259059156*^-7	-7922.56	1.06117
198	iron-56	492.2581	1.4073505540421094*^-7	-7766.05	1.06144
199	manganese-55	482.0743	1.5267284190077304*^-7	-7566.14	1.06175
200	chromium-54	474.0074	1.647089545988179*^-7	-7403.56	1.06204
201	iron-54	471.7626	1.6596411342311088*^-7	-7364.92	1.06207
202	chromium-53	464.2882	1.789572091626121*^-7	-7213.24	1.06236
203	chromium-52	456.3491	1.935505728689668*^-7	-7054.12	1.06267
204	vanadium-51	445.8446	2.1158206805627888*^-7	-6852.03	1.06302
205	titanium-50	437.7809	2.296789802598713*^-7	-6692.17	1.06334
206	chromium-50	435.0490	2.3199306572872738*^-7	-6646.05	1.06339
207	titanium-49	426.8417	2.5243387635161743*^-7	-6484.63	1.06373
208	titanium-48	418.6993	2.7508460278021466*^-7	-6324.95	1.06408
209	titanium-47	407.0727	3.044395166522623*^-7	-6108.04	1.0645
210	calcium-46	398.7687	3.332888821948236*^-7	-5947.34	1.06487
211	titanium-46	398.1924	3.340630153362403*^-7	-5937.82	1.06488
212	scandium-45	387.848	3.6956830432475527*^-7	-5744.39	1.06531
213	calcium-44	380.959	4.039212201815299*^-7	-5608.5	1.06569
214	calcium-43	369.8283	4.505058997638188*^-7	-5404.26	1.06617
215	calcium-42	361.8955	4.968151856130452*^-7	-5252.93	1.0666
216	potassium-41	351.6185	5.550654866568811*^-7	-5064.78	1.0671
217	argon-40	343.8104	6.148573047183578*^-7	-4917.13	1.06756
218	calcium-40	342.0520	6.199498749564236*^-7	-4889.16	1.0676
219	potassium-39	333.724	6.903540853520189*^-7	-4734.23	1.06809
220	argon-38	327.3424	7.635587940528749*^-7	-4610.71	1.06856
221	chlorine-37	317.100	8.633315978836048*^-7	-4427.5	1.06914
222	sulfur-36	308.7139	9.70305332372951*^-7	-4274.35	1.06971
223	argon-36	306.7167	9.805133626261248*^-7	-4243.48	1.06976
224	chlorine-35	298.2097	1.1067449574609924*^-6	-4089.67	1.07035
225	sulfur-34	291.8390	1.2389367244969239*^-6	-3969.38	1.07092
226	sulfur-33	280.4219	1.431995888076745*^-6	-3773.48	1.07165
227	sulfur-32	271.7803	1.6365022299416028*^-6	-3620.92	1.07234
228	phosphorus-31	262.9165	1.8809790589998228*^-6	-3466.22	1.07308
229	silicon-30	255.6196	2.1507782696164147*^-6	-3335.75	1.0738
230	silicon-29	245.0104	2.524553468404122*^-6	-3158.05	1.07468
231	silicon-28	236.5368	2.9387945510938122*^-6	-3012.89	1.07554
232	aluminum-27	224.9517	3.5181356739366058*^-6	-2824.85	1.07658
233	magnesium-26	216.6807	4.141440447802327*^-6	-2685.64	1.07755
234	magnesium-25	205.5876	5.017418557155385*^-6	-2508.7	1.07872

	nucleus	$E_b$ , MeV	$a_0$	$\mu_0$ , MeV	$Z(a_0)$
235	magnesium-24	198.2570	5.947104327628376*^-6	-2385.55	1.07979
236	sodium-23	186.5643	7.3726595268824775*^-6	-2204.77	1.08118
237	neon-22	177.7702	9.004247887526133*^-6	-2065.3	1.08252
238	neon-21	167.4060	0.000011278	-1907.2	1.08408
239	neon-20	160.645	0.0000137867	-1797.91	1.08552
240	fluorine-19	147.8013	0.0000181908	-1613.19	1.0876
241	oxygen-18	139.8064	0.0000231207	-1492.4	1.08948
242	oxygen-17	131.7624	0.0000298319	-1372.96	1.09156
243	oxygen-16	127.6193	0.000037166	-1301.73	1.09344
244	nitrogen-15	115.4919	0.0000524134	-1138.33	1.09654
245	nitrogen-14	104.6586	0.0000747585	-994.387	1.09996
246	carbon-13	97.10804	0.000104117	-890.48	1.10337
247	carbon-12	92.16173	0.000142128	-816.441	1.10679
248	boron-11	76.20482	0.000250039	-632.035	1.11361
249	boron-10	64.75071	0.000431932	-501.639	1.12108
250	beryllium-9	58.16482	0.000701309	-422.426	1.12854
251	lithium-7	39.24404	0.00289812	-229.33	1.15642
252	lithium-6	31.99407	0.00664184	-160.43	1.1785
253	helium-4	28.29566	0.0297622	-99.4456	1.23547
254	deuterium	2.224566	141873.	26.3893	5.06958

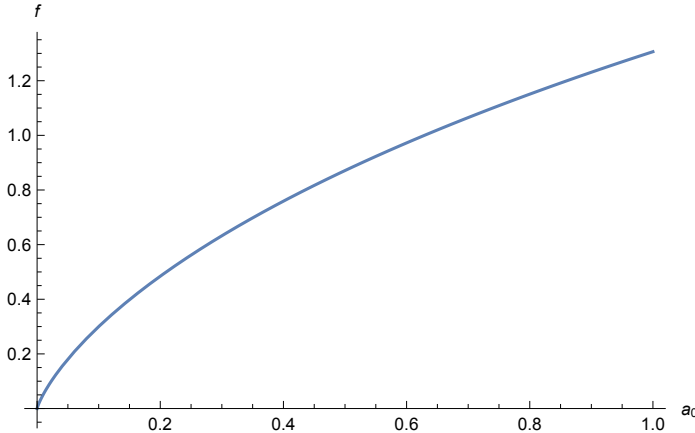


Figure 6: The dependence of the left hand side of the equation (59) on  $a_0$

Here  $E_b$  is the binding energy of the nucleus, equal to the core temperature  $T$ . It is well known that the binding energy of a nucleus increases with increasing mass number  $A$ . At the same time, the mass of the nucleus  $m$  and its volume  $V$  also grow. The equation (49) for  $\gamma = 1/2$  can be written as follows:

$$\frac{1}{2} \text{Li}_{3/2}(a_0) - \log(a_0) \text{Li}_{1/2}(a_0) = \frac{1}{V} \left( \frac{2\pi\hbar^2}{mT} \right)^{3/2}. \quad (59)$$

The value  $a = a_0$  is the minimum value of activity for the Bose branch, since for  $a < a_0$  the region of uncertainty occurs where  $N \equiv 0$  and  $P \equiv 0$  for all  $a$  up to the value of  $a = 0$ . Here the passage to the Fermi branch begins. Hence  $a_0$  is the point separating the Bose case from the case of uncertainty.

The left hand side of Eq. (59) which we denote by  $f(a_0)$  decreases when the value of  $a_0$  decreases (see Fig. 6). The value in the right hand side of (59) also decreases with the growth of the nucleus mass number  $A$ .

Therefore, as one can see from the Table, the activity  $a_0$  decreases and the absolute value of the chemical potential  $|\mu_0| = T|\log a_0|$  increases when the mass number  $A$  increases.

Thus we have obtained a new table for nuclear physics which demonstrates a monotonic relation between the nucleus mass number  $A$ , the binding energy  $E_b$ , the minimum value of activity  $a = a_0$ , the chemical potential  $\mu_0 = T \log a_0$ , and the compressibility factor  $Z = PV/NT$  for  $a_0$ .